

1 Coverage Methods for Early Groundwater Contamination 2 Detection

3

Luís Miguel Nunes¹ Faculty of Sciences and Technology, University of
Algarve, Faro, Portugal. e-mail: lnunes@ualg.pt
Maria da Conceição Cunha University of Coimbra, Coimbra, Portugal. e-mail:
mccunha@dec.uc.pt
Luís Ribeiro Instituto Superior Técnico, Lisbon Technical University,
Lisboa, Portugal. e-mail: luis.ribeiro@ist.utl.pt

4 **Abstract** A method based on space-filling coverage designs to optimize groundwater
5 monitoring networks for plume detection and quantification is proposed. Space-filling
6 objective functions are then compared with more classical functions. The method was
7 applied to a hypothetical case-study with 160 candidate locations, resulting in final
8 optimal design monitoring networks with 40 locations. Results show that the method is
9 superior to those based strictly on the probability of contamination detection for
10 quantifying maximum and mean values. In the light of these results fractal properties of
11 space-filling coverage methods and of simulated annealing are also discussed.

12 **Keywords:** space-filling, groundwater, monitoring

13

14

15 A vast number of technical documentation has been published on the design and
16 operation of groundwater monitoring networks, namely in respect to where monitoring
17 points should be located and which sampling strategies to adopt. Four techniques are used
18 to tackle these questions. The first is based on geostatistical methods (Rouhani 1985), and
19 the second on simulation methods, also from the late 1980s (Massmann and Freeze
20 1987). The third category of techniques to appear involved transfer functions (Andricevic
21 1990). However, the most widely used approaches are optimization methods, which were
22 first introduced in the early eighties (Olea 1999), being latter developed by many other
23 authors, with the later models gradually incorporating objective functions with cost
24 parameters, such as, installation, operation, maintenance and environmental costs (Reed
25 *et al.* 2000), or the minimization of the number of wells (Meyer *et al.* 1994). A detection
26 monitoring network is optimal if its capacity to detect early contamination is maximal
27 (Meyer *et al.* 1994) and the concentration levels are very low. A compliance monitoring
28 network is one that is able to give the best representation of the effective concentrations –
29 best represents the spatial distribution of the variable (Cunha and Nunes 2011). Some
30 simplifications to least-cost objective functions have been proposed, in particular by
31 using proxies, like minimizing the error of kriged concentration values, or the variance of
32 the error of the kriged concentration error (Nunes *et al.* 2004b). We concentrate here on
33 another proxy method, the space-filling methods, for which this is the first application in
34 groundwater monitoring. Space-filling functions have already been used in the design of

¹ Corresponding author

35 air quality monitoring network design by Morris and Mitchell (1995) and by Royle and
36 Nychka (1998). As the decision variables (location of the monitoring site) are
37 combinatorial, the models contain discrete variables and so the classic linear, nonlinear
38 and integer linear programming methods are unsuitable. Lee and Ellis (1996) concluded
39 that simulated annealing and tabu search perform best for groundwater monitoring
40 network design.

41
42 One of the hardest tasks in groundwater contamination evaluation is to characterize
43 contamination plumes, because a large number of sampling sites is generally required to
44 obtain good estimates (accurate and exact) of the contaminated area and concentration
45 values. The practical difficulty with these estimates is directly related to the uncertainty
46 about many of the flow and transport parameters. At the top of the list are the medium's
47 hydraulic conductivity and dispersivity. Hydraulic conductivity affects groundwater flow
48 velocities at all scales, which, as a result, will also condition contaminant dispersion
49 (calculated as the product of flow velocity and dispersivity). These uncertainties about
50 parameters (state-variables) should be incorporated into the modeling to best reflect
51 uncertain decisions about parameter values. The uncertainty is well handled by statistical
52 approaches, where a state-variable spatial distribution is considered a random function,
53 the value at a given location is a random variable, and the sampled values are a possible
54 outcome of the random variable. There are two main approaches to groundwater
55 modeling using random fields of medium parameters. One is the expansion of the
56 uncertain parameters in terms of a series. The other is stochastic simulations based on
57 Monte Carlo methods, of which the most common are Latin hypercube sampling,
58 sequential Gaussian simulations, turning bands method, and LU decomposition.

59
60 In the present paper a method for optimizing monitoring networks for detecting and
61 estimating the shape of the plumes is presented. The method combines space-filling
62 methods and Monte-Carlo sequential simulations. Two objective functions are compared:
63 i) includes both the space-filling criterion and the relative number of contamination
64 detections criterion; ii) includes only the relative number of contamination detections
65 criterion. The latter is similar to the objective functions proposed by other authors as the
66 "probability of contamination detection" criterion (James and Gorelick 1994). A specific
67 computed code in FORTRAN was developed by the team to test monitoring optimization
68 problems. Some very preliminary results were presented in Nunes *et al.* (2005).

69
70

71 **Materials and methods**

72 The method requires the simulation of L alternative concentration fields by modeling mass
73 transport in an equal number of hydraulic conductivity random fields, in which Ω
74 locations are placed (Step 1) – candidate set \mathbf{C} ; in Step 2 a set of ω locations is chosen
75 from \mathbf{C} , generating design set \mathbf{D} (solution generation); in Step 3 the number of detections
76 and the space-filling criterion are computed using the design set, and the objective
77 function (OF) is computed. Convergence of the objective function to the optimal value is
78 controlled by the simulated annealing algorithm, responsible for controlling the entire
79 process starting in Step 2: the process of solution generation and OF calculation is

80 cyclical until the criteria for stopping the algorithm are attained and the optimal solution
 81 presented (see Figure 1).

82

83

84 **Figure 1 Method**

85

86 The candidate sets \mathbf{C} are obtained by making mass transport simulations of contaminant
 87 dispersion in groundwater and considering the sampling locations as the values in the
 88 model nodes. Uncertainty is introduced by generating several conditional simulations of
 89 the hydraulic conductivity field using sequential Gaussian simulation. The method is
 90 conveniently offered by the GSLIB geostatistical toolbox (Deutsch and Journel 1992).
 91 Applying the deterministic groundwater flow to these random fields will result in
 92 hydraulic potential fields and velocity fields that are also random functions. Solving flow
 93 and transport equations with the proper initial and boundary conditions simulates the
 94 transport of a chemical species. If enough stochastic simulations are computed and
 95 modeled, then it will be possible to compute, at each model cell, the density function of
 96 contaminant concentration, and also the probability that a given threshold is surpassed.
 97 Consider the concentration of a chemical species study, $C(x_{i,j})$, at a location $x_{i,j}$, and a
 98 reference value (e.g., legal limit, or analytical detection limit), C_{ref} , then, the relative
 99 number of detections is determined by

$$a_m(x_{i,j}) = \begin{cases} 1 & \text{if } C_m(x_{i,j}) \geq C_{ref} \\ 0 & \text{otherwise} \end{cases} \quad m = 1, \dots, L \quad (3)$$

$$r(x_{i,j}) = \frac{1}{L} \sum_{m=1}^L a_m(x_{i,j})$$

100 The use of $r(x_{i,j})$ reflects the empirical need to include in the monitoring network those
 101 stations that detected contamination more often, i.e., with higher detection capacity. A
 102 good space-filling design is one with monitoring locations scattered throughout the
 103 domain with minimal unsampled areas (Fang *et al.* 2000). Space-filling methods use a
 104 criterion based on a metric that makes it possible to evaluate the goodness of a space
 105 covering design. The most common criteria are based on the average of distances
 106 between candidate locations and the locations already included in the design sub-set
 107 (equation (4)). One possible metric is given by $d_p(x, \mathbf{D})$.

$$\Pi_{p,q}(\mathbf{D}) = \left(\sum_{u \in \mathbf{C}} d_p(x, \mathbf{D})^q \right)^{1/q}, \quad \text{with} \quad d_p(x, \mathbf{D}) = \left(\sum_{u \in \mathbf{D}} \|x - u\|^p \right)^{1/p} \quad (4)$$

108 The exponent q is >0 and is $p < 0$. $d_p(x, \mathbf{D}) \rightarrow 0$ as the location x converges to a member of
 109 \mathbf{D} . The coverage design is the subset of ω elements in \mathbf{D} from the Ω elements in \mathbf{C} , $\mathbf{D} \subset \mathbf{C}$,
 110 that minimize the criterion $\Pi_{p,q}(\mathbf{D})$. The algorithm implemented in our computer code
 111 is a simulated annealing equivalent of the exchange (or swap) algorithm as proposed by
 112 Johnson *et al.* (1990) considering no restriction on neighborhood search. The two
 113 objective functions studied here are

$$(M1) \quad \min \frac{\Pi_{p,q}(\mathbf{D})}{\sum_i \sum_j r(x_{i,j})} \quad (5)$$

$$(M2) \quad \max \sum_i \sum_j r(x_{i,j})$$

114 M1 was constructed so as to combine the best characteristics of the “probability of
 115 contamination detection” criterion, and the space-filling criterion. With the first,
 116 maximization of contamination detection is sought; with the second criterion,
 117 maximization of space coverage is intended. Hence, the resulting monitoring networks
 118 should allow good estimates of contaminated areas, and good contamination detection
 119 capacity. M2 has been used by many other authors in other methodological approaches,
 120 and is used here for benchmarking the first model. The problem proposed here was
 121 solved using a simulated annealing (SA) heuristic optimization algorithm, executed in
 122 Fortran 90. The implementation followed the description presented in Nunes et al.
 123 (2004a).

124

125 The proposed objective function models were tested in a hypothetical case-study,
 126 consisting of a continuous source of a conservative chemical species, located in a very
 127 small area, which contaminates a porous unconfined aquifer. This example illustrates,
 128 e.g., the leakage from storage tanks, or from landfills, of a chemical species that does not
 129 adsorb to the soil matrix nor is it affected by degradation, or does so in a very limited
 130 fraction. The problem usually faced in these cases is where to locate the monitoring
 131 piezometers so that they have the greatest probability of detecting the contamination, also
 132 allowing the best estimation of the plume concentration geometry (estimation of the
 133 affected area and volume). The problem that is solved here is one of detection and
 134 evaluation of spread monitoring after the early detection of a rupture in an underground
 135 containment structure, or a spill on the soil surface. The period between leakage and
 136 setting of the monitoring network for early assessment of contamination is 30 days,
 137 corresponding to the amount of time elapsing between first detection, decision to
 138 undertake the monitoring, contracting the service, and setting up the monitoring network.
 139 The modeling domain is, in this simplified example, a rectangle of 400 m x 150 m,
 140 discretized into a 10 m squared mesh, in 2D conditions. Upper and lower limits of the
 141 porous medium are horizontal and the depth of the aquifer is 20 m. Flow boundary
 142 conditions of Dirichlet type with a head value at 27 m on the West boundary and at 24 m
 143 on the East boundary. No pumping and no recharge are considered. Simulation time is 30
 144 days. Given the fact that modeling conditions do not change during the modeling period,
 145 steady-state conditions are used. Hydraulic conductivity is a heterogeneous stochastic
 146 field with mean hydraulic conductivity, K , of 2.12×10^{-2} m/s, and variance of hydraulic
 147 conductivity of 2.5×10^{-1} m²/s², modeled with an isotropic spherical variogram (nugget =
 148 0.01; sill = 0.24; range = 80 m). Effective porosity is considered constant and equal to 0.1
 149 throughout the domain, whatever the value of K . The longitudinal dispersivity coefficient
 150 is 4.5 m, with anisotropy ratio, α_y/α_x , of 0.25. The amount of the chemical species
 151 entering at the top the water table is 400 g/m².d, modeled as a contaminated recharge over
 152 an area of 100 m². No retardation or degradation is considered (given the short time
 153 length considered, the latter assumption is valid even for the most readily biodegradable
 154 species). The molecular diffusion coefficient is considered irrelevant, given the
 155 groundwater flow velocity. At the onset of the simulation concentrations of the chemical

156 species inside the domain are zero. Groundwater potentials (equation (1)) in the domain
157 are simulated with MODFLOW (McDonald and Harbaugh 1988). Concentrations are
158 simulated with the MT3D code (Zheng 1990), which solves equation (2) for conservative
159 chemical species. Calculation of the value of $r(x_{i,j})$ required carrying out 100 stochastic
160 sequential Gaussian simulations and an equal number of flow and mass transport
161 simulations. The reference value, C_{ref} , is 50 mg/l. It is assumed that the candidate set of
162 locations is known, with dimension Ω , and that a design sub-set, with dimension ω , is
163 sought. The design problem is to find the optimal set of ω locations, $\mathbf{D}=(x_i : i=1,2, \dots,$
164 $\omega)$, from a candidate set with Ω locations, $\mathbf{C}=(x_j : j=1,2, \dots, \Omega)$. The candidate set has
165 $\Omega=160$ locations, of which only $\omega=40$ locations are allowed in the optimal design
166 monitoring network. The dimension of the solution space is given by the well-known
167 equation $\Psi=\Omega!/[(\Omega-\omega)! \omega!]=8.6 \times 10^{37}$.

168

169 **Results and Discussion**

170 The objective function model M1 was studied for four different combinations of the
171 coefficients p and q : $n(p,q)=((-1,3),(-1,4),(-3,2),(-3,4))$. The choice of the coefficients is
172 arbitrary. For instance, Royle and Nychka (1998) used $p=-5$ and $q=-1$, as a compromise
173 between designs that are close to the minimax solution. In our case the combination $(-5,-$
174 $1)$ was found to be too instable to compute, giving no meaningful results in any of the 10
175 runs. It will be clear that for some combinations of p and q the convergence is much more
176 difficult or even impossible in a practical amount of time. The results from the tested
177 objective functions were compared with OF M2 to evaluate the impact of including the
178 space-filling component in the objective function. If the problem had had to be solved
179 exhaustively by testing all the possible combinations of locations it would require, with
180 the 2GHz Pentium PC used in the calculus, more than 6.9×10^{29} years. The solutions
181 presented here, which are the best from 10 runs with different initial solutions, took
182 nearly 7 hours to calculate each. When the algorithm converges, SA has been found to be
183 an efficient optimization method. The disadvantage is that it is impossible to know if the
184 good quality solution obtained by the algorithm is the global optimum (the minimum of
185 the minima), because optimality is only guaranteed in an almost infinite number of
186 iterations (almost infinite time). The advantages far outweigh the disadvantages, though.
187 Figure 2 shows the convergence curves for two (p,q) combinations. A large jump from
188 high objective function values at high temperatures to very low values is evident for $(-$
189 $1,3)$. Since simulated annealing is a method based on physics annealing processes, when
190 a material is cooled slowly into its crystallized form it is possible that it may show some
191 characteristics also common in physics, like supersolid transition: a very fast drop in
192 some characteristic of the material when cooled to below some critical temperature
193 (Andreev and Lifshitz 1969). This may also be related to fractal properties of space-
194 filling networks, for which there seems to be a constant factor relating the dimension of
195 the network (distance between locations or number of branches in a network) to its
196 coverage area. What may be happening here is that the critical temperature is related in
197 some way to specific spatial organizations that best approximate the fractal nature
198 governing natural networks. This may become an important indication as to which
199 solutions may be the best candidates to constitute a smaller solution space, if one can
200 devise a method to identify a set of solutions with the correct fractal nature (e.g., similar
201 fractal dimension). The behavior of simulated annealing depends crucially on the energy

202 landscape associated with the optimization problem: the landscape must have special
203 properties if annealing is to be efficient (fractalness) (Sorkin 1991). Figure 2 shows that
204 for (-2,3) the fractalness may not have been found, indicating that either a different
205 transition rule could have been used to improve further the solution (e.g., 2 or 3-opt),
206 and/or a different combination of this with a slower temperature decrease, but at the
207 expense of longer running times. These results do not explore all possible combinations
208 of M1 objective functions (nor is that possible), but they do show that it may be advisable
209 to test some different objective functions before choosing a solution. For comparison
210 purposes both the random field $r(x_{i,j})$ obtained with the candidate sets \mathbf{C} , $r_{\mathbf{C}}(x_{i,j})$ and those
211 obtained with the optimal \mathbf{D} sets, $r_{\mathbf{D}}(x_{i,j})$, were kriged in an area equal to the modeling
212 domain, in a grid with $15 \times 39 = 585$ nodes, using the same variogram model as before.
213 The kriged fields were then compared with the following statistics: i) mean; ii)
214 maximum; iii) minimum; iv) mean estimation error; v) relative mean error $[(r_{\mathbf{D}}(x_{i,j}) -$
215 $r_{\mathbf{C}}(x_{i,j}))/585]$; vi) mean estimation variance. When comparing the two solutions that
216 converged, $(p,q)=(-1,3)$ or $(-2,3)$, with the other two that did not (not shown in the
217 figure), it is clear that in terms of the quality of the reproduction of the spatial field, the
218 former outperform the latter. This is indicated by a mean estimated $r_{\mathbf{D}}(x_{i,j})$ value closer to
219 that of the candidate network, $r_{\mathbf{C}}(x_{i,j})$. It is interesting to see that the statistics (Table 1) for
220 $(p,q) = (-3,4)$ are all at a very good level, with the exception of the mean estimated value,
221 which is the worst of the four, and so the solution would have been a good one in a strict
222 variance-reduction approach.

223

224 **Table 1** Comparison of results for objective functions M1 and M2 (best of the ten runs)

225

226 Results showed that if the intuitive approach of including stations in the design is
227 exclusively based on the highest relative number of detections (M2), the resulting
228 network will tend to be too concentrated in the center of the plume (Figure 3c). Also in
229 this case the quality of the estimated spatial field (of $r(x_{i,j})$) (and therefore of the
230 concentrations) is very poor, as shown by the indicator statistics in Table 1. This
231 objective function has the worst results of the five.

232

233 **Figure 2** Simulated annealing convergence curves (best of the ten runs)

234

235 If the objective function M1 is used, the network is much more evenly distributed in
236 space, covering not only the center of the plume, but also areas where contamination
237 levels are very low (see Figure 3). This is usually a much more realistic objective when
238 dealing with the detection of contamination events from point or areal sources. Other
239 methods have been proposed along these lines using geostatistics and exploration costs
240 by (Cunha and Nunes 2011) with similar results. The advantage of the space-
241 filling/relative number of detections method over the variance-reduction method lies in its
242 speed, because geostatistical simulations are made before the optimization, no kriging is
243 needed during optimization, and because it is not constrained by ergodicity assumptions
244 (not always verified in contaminated areas due to three-dimensional concentration
245 trends).

246

247

248 **Figure 3** a) Relative number of detections, $r_C(x_{i,j})$; b) M1; c) M2

249

250 The advantages over other methods is the simplicity and speed of its implementation, as
251 well as its intuitively more reality-based approach, making it easier to convey to decision
252 makers. It describes a method for optimizing monitoring networks for the detection and
253 estimation of the shape of the plumes. The intuitive approach of including stations in the
254 design exclusively based on the highest relative number of detections resulted in a
255 monitoring network that is too concentrated in the center of the plume. If the objective
256 function M1 is used, the network was revealed to be much more evenly distributed in
257 space, covering not only the center of the plume, but also areas where contamination
258 levels are very low. This is a much more realistic result when dealing with the detection of
259 contamination events from point or areal sources.

260

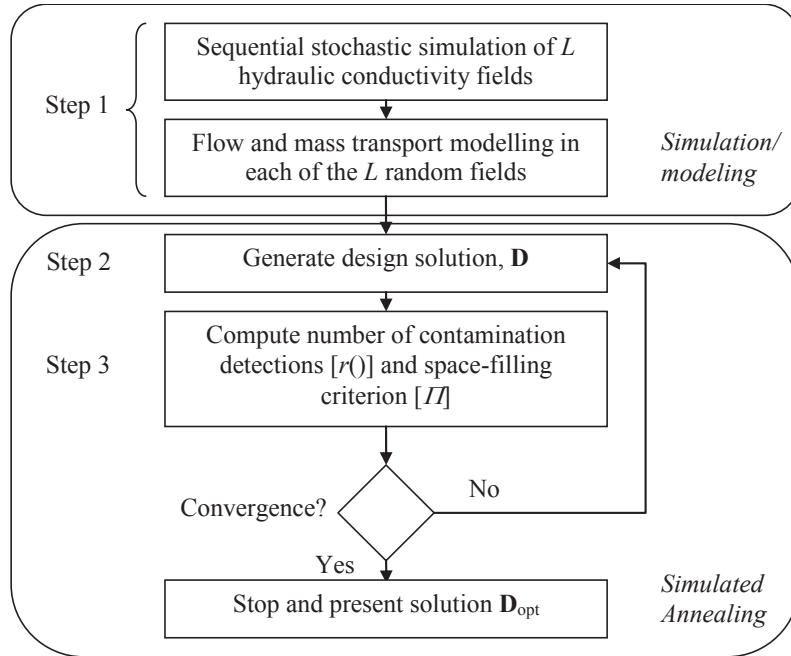
261 **References**

- 262 Andreev AF, Lifshitz IM (1969) Quantum theory of defects in crystals. *Sov Phys JETP-*
263 *USSR* 29: 1107-1113
- 264 Andricevic R (1990) Cost-effective network design for groundwater-flow monitoring.
265 *Stoch Hydrol Hydraul* 4(1): 27-41
- 266 Cunha MC, Nunes LM (2011) *Groundwater systems: characterization, management and*
267 *monitoring*. WIT Press, Southampton, UK
- 268 Deutsch, CV, AG *Journel* (1992) *GSLIB - Geostatistical software library and user's*
269 *guide*. Oxford University Press, New York, USA
- 270 Fang, KT, Lin DKJ, Winker P, Zhang Y (2000) *Uniform Design: Theory and*
271 *Application*. *Technometrics* 42(3): 237-248
- 272 Johnson ME, Moore LM, Ylvisaker D (1990) Minimax and maximin distance designs. *J*
273 *Stat Plan Infer* 26: 131-148
- 274 Lee YM, Ellis JH (1996) Comparison of algorithms for nonlinear integer optimization:
275 application to monitoring network design. *J Environ Eng-ASCE* 122(6): 524-531
- 276 Massmann J, Freeze RA (1987) Groundwater contamination from waste management
277 sites: the interaction between risk-based engineering design and regulatory policy, 1.
278 *Methodology*. *Water Resour Res* 23(2): 351-367
- 279 McDonald MG, Harbaugh AW (1988) A modular three-dimensional finite-difference
280 ground-water flow model. Book 6, United States Geological Survey, USA
- 281 Meyer PD, Valocchi AJ, Eheart JW (1994) Monitoring network design to provide initial
282 detection of groundwater contamination. *Water Resour Res* 30(9): 2647-2659
- 283 Morris MD, Mitchell TJ (1995) Exploratory designs for computational experiments. *J*
284 *Stat Plan Infer* 43: 381-402
- 285 Nunes LM, Cunha MC, Ribeiro L (2004a) Groundwater monitoring networks
286 optimization with redundancy reduction. *J Water Res PL - ASCE* 130(1): 33-43
- 287 Nunes LM, Cunha MC, Ribeiro L (2004b) Groundwater nitrate monitoring network
288 optimization with missing data. *Water Resour Res* 40(2): 1-18
- 289 Nunes LM, Cunha MC, Ribeiro L, Azevedo J (2005) New method for groundwater
290 plume detection under uncertainty. In: *Water in Celtic Countries: Quantity, Quality and*
291 *Climate Variability, The Fourth Inter-Celtic Colloquium on Hydrology and Management*
292 *of Water Resources, July 11-13, 2005, Guimarães, Portugal*
- 293 Olea RA (1999) *Geostatistics for Engineers and Earth Scientists*. Springer, New York

294 Reed P, Minsker B, Valocchi AJ (2000) Cost-effective long-term groundwater
295 monitoring design using a genetic algorithm and global mass interpolation. *Water Resour*
296 *Res* 36(12): 3731-3741
297 Rouhani S (1985) Variance reduction analysis. *Water Resour Res* 21(6): 837-846
298 Royle JA, Nychka D (1998) An algorithm for the construction of spatial coverage designs
299 with implementation in SPLUS. *Comput Geosci-UK* 24(5): 479-488
300 Sorkin GB (1991) Efficient simulated annealing on fractal energy landscapes.
301 *Algorithmica* 6: 367-418
302 Zheng C (1990) MT3D: A modular three-dimensional transport model for simulation of
303 advection, dispersion and chemical reactions of contaminants in ground water systems. S.
304 S. Papadopulos and Assoc, USA.
305
306

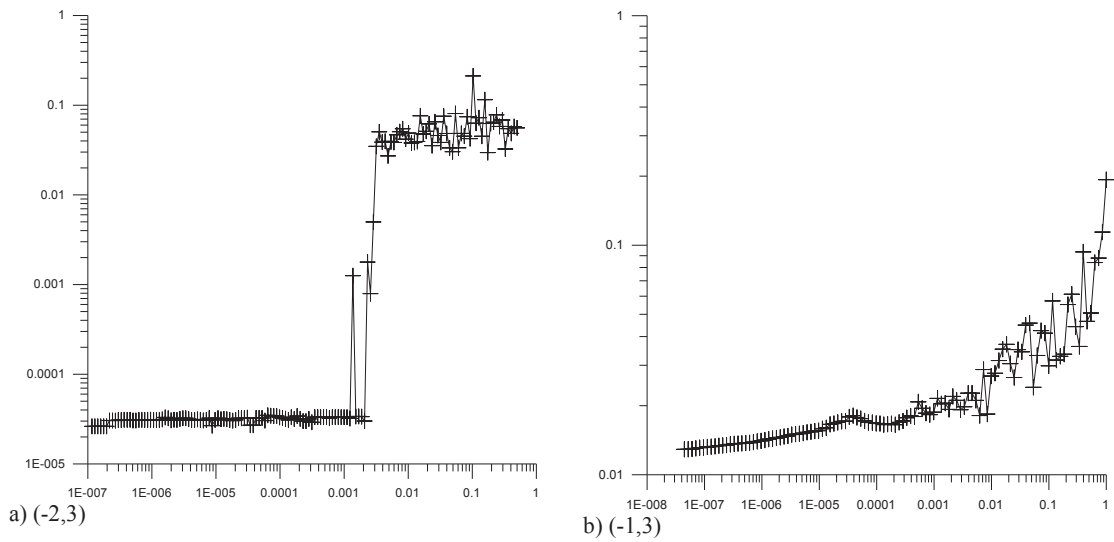
307
308
309

FIGURES



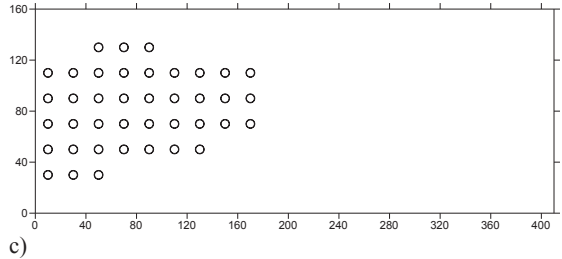
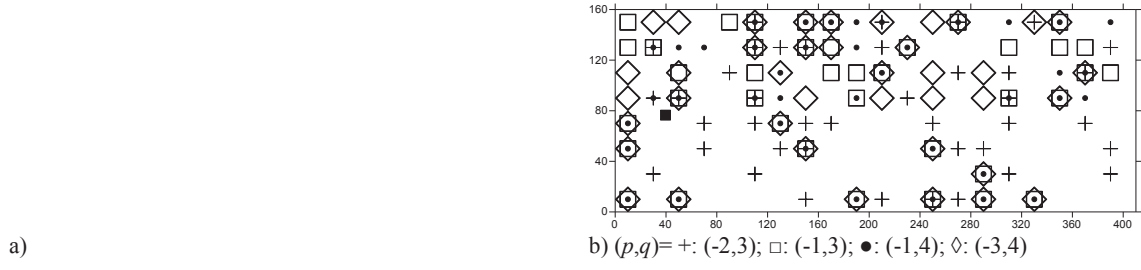
310
311
312
313

Figure 1. Method



314
315
316

Figure 2. Simulated annealing convergence curves (best of the ten runs)



317 Figure 3. a) Relative number of detections, $r_C(x_{i,j})$; b) M1; c) M2
 318
 319
 320

321

322 TABLES

323

324

325 Table 1. Comparison of results for objective functions M1 and M2 (best of the ten runs)

Indicators	$r_c(x_{i,j})$	M2 [$r_D(x_{i,j})$]	M1 [$r_D(x_{i,j})$]			
			$p=-1; q=3$	$p=-1; q=4$	$p=-2; q=3$	$p=-3; q=4$
Mean	0.2970	0.24565	0.26572	0.26578	0.29538	0.26475
Maximum	0.7143	0.6780	0.7080	0.7080	0.7080	0.7080
Minimum	0.0	0.0	0.0	0.0	0.0	0.0
Mean error	-0.00074	-0.00205	0.00456	0.00668	0.00508	0.00425
Relative mean error	-	0.00830	0.0172	0.0251	0.0172	0.0161
Mean Estimation Variance	0.00240	0.0054	0.0053	0.0054	0.0056	0.0053
Rank	-	3	2	-	1	-

326